ESMO GOOD SCIENCE BETTER MEDICINE BEST PRACTICE

IOTECH IMMUNO-ONCOLOGY TECHNOLOGY

REVIEW

Nanobodies as non-invasive imaging tools

M. Rashidian[1*] **& H. Ploegh**[2*]

[1]Dana-Farber Cancer Institute, Harvard Medical School, Boston; [2]Program in Cellular and Molecular Medicine, Boston Children's Hospital, Harvard Medical School, Boston, USA

Available online 9 July 2020

Antibodies and antibody fragments have found wide application for therapeutic and diagnostic purposes. Single-domain antibody fragments, also known as 'heavy-chain variable domains' or 'nanobodies', are a recent addition to the toolbox. Discovered some 30 years ago, nanobodies are the smallest antibody-derived fragments that retain antigen-binding properties. Their small size, stability, specificity, affinity and ease of manufacture make them appealing for use as imaging agents in the laboratory and the clinic. With the recent surge in immunotherapeutics and the success of cancer immunotherapy, it is important to be able to image immune responses and cancer biomarkers non-invasively to allocate resources and guide the best possible treatment of patients with cancer. This article reviews recent advances in the application of nanobodies as cancer imaging agents. While much work has been done in preclinical models, first-in-human applications are beginning to show the value of nanobodies as imaging agents.

Key words: nanobody, ImmunoPET, non-invasive imaging, immunotherapy, cancer biomarkers, PET imaging

INTRODUCTION

The ability to visualize biological processes in a living animal and to be able to diagnose aberrations, such as developmental abnormalities or signs of disease, have always been desirable goals. This has spawned the development of many different imaging modalities, ranging from conventional microscopy methods, aimed at single cells and multiphoton intravital microscopy, to non-invasive methods at the organismal level, such as magnetic resonance imaging, computed tomography (CT), positron emission tomography (PET), single-photon emission computed tomography (SPECT), bioluminescence and ultrasound imaging. There is still a dearth of methods to look inside the living organism and visualize specific markers with adequate resolution and specificity. Imaging is essential to make the correct clinical decisions for many diseases, including cancer, The presence or absence of particular biomarkers in the tumor microenvironment (TME), on immune infiltrating cells, and in the extracellular matrix (ECM) of tumors may inform the choice of optimal treatment options.

Immunotherapy has revolutionized cancer treatment.[1–3] However, only a fraction of patients respond, and some patients experience severe side-effects. Immunotherapy trials are hampered by a lack of adequate methods to monitor responses non-invasively. There are currently no reliable biomarkers to stratify cohorts into responders and non-responders soon after the start of treatment. A detailed characterization of immune infiltrates will be crucial to understand why so many patients with cancer do not respond to immunotherapy and, more importantly, what measures can be developed to improve the prospects for such interventions. Standard imaging approaches do not always distinguish between a growing tumor and an increase in mass attributable to a robust immune response with the attendant expansion in cell numbers.[4] Thus, the ability to evaluate the presence and distribution of the immunological checkpoint molecules, such as PD-1/PD-L1[1,5] and CTLA-4,[6] of markers such as CD4 and CD8 on T cells,[7,8] or to register the presence of macrophages[9] will enhance the diagnostic toolbox. The ultimate goal is to be able to monitor, and possibly predict, the clinical behavior of the appropriate patient populations without having to resort to undesirable invasive procedures.

The presence or absence of specific markers on primary tumors or their metastatic lesions can help make informed treatment decisions, such as whether or not to consider immunotherapy as a treatment option. Biopsies, followed by histology and immunohistochemistry, remain the gold standard for the characterization of tumors. Biopsies, however, are prone to sampling errors. Moreover, tumors

*Correspondence to: M. Rashidian, Dana-Farber Cancer Institute, Harvard Medical School, Boston, MA 02115, USA. Tel: 857-215-5592
E-mail: Mohammad_Rashidian@dfci.harvard.edu (M. Rashidian).
*H. Ploegh, Program in Cellular and Molecular Medicine, Boston Children's Hospital, Harvard Medical School, Boston, MA 02115, USA. Tel: 617-919-1613
E-mail: Hidde.Ploegh@childrens.harvard.edu (H. Ploegh).

are often heterogeneous in cellular composition.[10–12] Therefore, biopsies rarely provide a complete picture of the TME. Metastatic lesions can differ significantly from each other in their molecular and immunological properties, and also from the primary tumor.[10,13–15] Performing biopsies on all lesions is often impractical and some lesions are not even accessible to biopsies.[16,17] Non-invasive imaging of the biomarkers could provide an alternative to address this.

ECM deposition and, especially, its modification are hallmarks of cancer.[18] Cancer cells make close contact with the ECM. The tumor ECM provides structural support, plays a role in survival and progression of cancer cells, and may affect the tumor response to treatment. We need to better understand how the ECM responds to various treatments, and how it affects the dynamics and the interplay between cancer cells and the immune infiltrating cells. Non-invasive imaging of the ECM components and how they change in response to treatment may help us to better understand the effect of the ECM on treatment outcome.

Imaging methods that can provide a whole-body scan, such as PET and SPECT, begin to establish a non-invasive approach to the characterization of a tumor in terms of its local environment and cellular composition. PET uses isotopes that emit a positron such as ^{11}C ($t_{1/2}$ ~20 min), ^{68}Ga ($t_{1/2}$ ~68 min), ^{18}F ($t_{1/2}$ ~110 min), ^{64}Cu ($t_{1/2}$ ~12.7 h) or ^{89}Zr ($t_{1/2}$ ~3.3 days). SPECT uses isotopes that emit gamma rays, such as ^{99m}Tc ($t_{1/2}$ ~6 h) or ^{111}In ($t_{1/2}$ ~67.3 h). PET is considered to be the more attractive imaging option because of its higher resolution, availability of positron-emitting isotopes, and the instrumentation available in most nuclear medicine departments.

The most commonly used radiotracer is ^{18}F-2-fluoro-2-deoxyglucose (^{18}F-FDG). Differences in glucose uptake allow differentiation of glucose-avid, rapidly proliferating cancer cells and their metastases from the surrounding tissues. ^{18}F-FDG fails to detect lesions that are less metabolically active or glucose avid, and this is a common problem of ^{18}F-FDG PET (false-negative results). ^{18}F-FDG PET can also uncover sites of inflammation, which can result in false-positive signals in patients with cancer. This lack of specificity can complicate the interpretation of ^{18}F-FDG PET images from cancer patients with autoimmune diseases, such as pulmonary vasculitis.[19] Other existing small molecule radiotracers, such as 3′-deoxy-3′[^{18}F]-fluorothymidine, suffer from similar non-specific uptake issues, although there are exceptions, such as 2-(3-{1-carboxy-5-[(6-[18F] fluoro-pyridine-3-carbonyl)-amino]-pentyl}-ureido)-pentanedioic acid[20] which targets prostate-specific membrane antigen and is currently in a phase III clinical trial (NCT03739684).

The use of antibodies can help to address the challenge of specificity. Antibodies can detect cancer-specific markers, and identify tumor-infiltrating immune cells or components of the tumor ECM. Antibodies exist for many cell-surface-available markers. In fact, one might go so far as to say that the human immune cell surface is among the best immunologically mapped in all of biology, based on the known numbers of CD antigens in comparison with all other species (>400 CD molecules at present[21]). PET using antibodies and antibody fragments as imaging agents is usually referred to as 'immunoPET'.[22–24] Radiolabeled antibodies or their fragments can be used to visualize and track location, movement and quantity of the target molecule, thereby providing insight into its dynamics.

When designing an imaging agent, several factors must be considered. Once a tracer is injected into the bloodstream, it must enter the tissue of interest and then bind to its target. A radiotracer's ability to penetrate the TME worsens with increased interstitial pressure inside the tumor. Differences in tracer accumulation between tumor lesions, or even within a single lesion, do not necessarily mean heterogeneity in expression of the target. A tracer may accumulate in a tissue without binding specifically to its target. Signal accumulation is considered specific when a 'cold' unlabeled tracer diminishes the signal of the actual imaging agent, or when a knockout cell line or animal shows an absence of signal. Furthermore, immunohistochemistry is needed to confirm specificity and characterize the sensitivity of a tracer.

The optimal non-invasive imaging agent would have high specificity and sensitivity, and show good tissue penetration to allow rapid imaging after injection. The patient's radiation exposure should be minimized and the need for a second visit should be avoided where possible. These parameters are only partly compatible. Full-sized antibodies as imaging agents best reflect the pharmacokinetics and pharmacodynamics of their therapeutic equivalents. Several preclinical and clinical studies have used full-sized therapeutic antibodies as imaging agents; examples include radiolabeled trastuzumab (anti-HER2 IgG), nivolumab (anti-PD-1 IgG) and atezolizumab (anti-PD-L1 IgG).[5,25–27] However, the use of full-sized antibodies for non-invasive imaging comes with drawbacks. The relatively long circulatory half-lives ($t_{1/2}$ of several days to weeks) of full-sized antibodies preclude the use of shorter-lived isotopes, such as ^{18}F, and instead require labeling with ^{89}Zr, necessitating rehospitalization and additional radiation exposure. Their considerable size (~150 kDa) can hinder efficient diffusion and/or tissue penetration.[28] Therefore, using an immunoglobulin G (IgG) as an imaging agent, especially when the full-sized antibody is not the drug itself, may not be the best choice. To address these drawbacks, radiolabeled antibody fragments have been developed. These include minibodies (~80 kDa, $t_{1/2}$ ~5–7 h), cys-diabodies (~60 kDa, $t_{1/2}$ ~2–4 h), antigen-binding fragments (Fab, ~50 kDa, $t_{1/2}$ ~2–4 h) and single-chain Fv fragments (~25 kDa, $t_{1/2}$ of ~30–60 min) (Figure 1).[29–32] These altered formats typically require a considerable engineering effort to achieve acceptable circulatory half-lives, stability and expression levels during the production phase. Nanobodies, as the smallest naturally derived antibody fragments that retain antigen binding, represent an attractive alternative (~15 kD, $t_{1/2}$ ~15 min, nM to pM affinity range[33,34]).

Camelids produce a subset of immunoglobulins composed of two identical heavy chains, each equipped

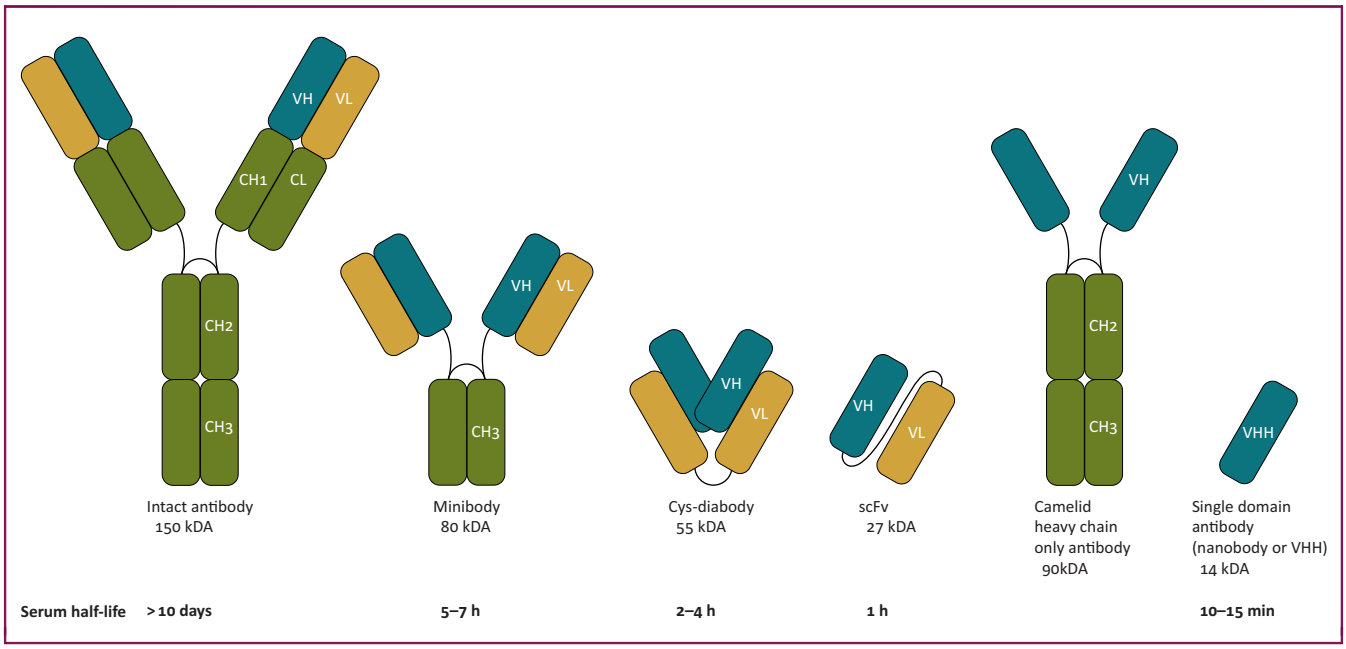

Figure 1. Representation of antibody and antibody fragments commonly used in positron emission tomography or single-photon emission computed tomography. VHH, heavy-chain variable domain.

with a heavy-chain variable domain (VHH) that binds antigen (Figure 1).[35] The VHH segments can be expressed recombinantly as small, highly water-soluble and stable proteins. To generate nanobodies, animals are immunized with (a) protein(s) of interest. The resulting repertoire of immune VHHs is cloned from peripheral blood lymphocytes, and used to generate a phage or yeast display library. VHHs specific for the antigen of interest are recovered; for example, by panning against the immobilized antigen. The relevant VHHs are then expressed recombinantly (Figure 2).[36] Several nanobodies have been produced and characterized as imaging agents (Table 1).

Several approaches have been developed to radiolabel antibodies and antibody fragments. Most methods rely on fairly non-specific labeling using N-hydroxysuccinimide, p-isothiocyanatobenzyl or maleimide derivatives; N-hydroxysuccinimide and p-isothiocyanatobenzyl react with free amines, and maleimide derivatives react with cysteine-free thiols. Non-specific labeling approaches typically yield chemically heterogeneous products with varying numbers of the installed tags, and may damage the antibody's binding site. For clinical translation, a homogeneous, well-defined product would be preferable. When smaller antibody fragments, such as nanobodies, are used, the radioisotope will be installed closer to the binding site, with an increased chance of damaging the antibody's paratope (i.e. the portion of the molecule via which it binds to its cognate antigen). Ideally, the radioisotope should be installed distal to the binding site. Crystallography shows that the paratope of nanobodies is opposite the C-terminus.[75] Thus, several site-specific modification approaches have been developed to modify the nanobodies at their C-terminus. A C-terminal His6-tag has been used to install ^{99m}Tc, an SPECT isotope (Figure 3).[44,76] Several enzymatic methods can be used to modify proteins and antibodies at a specific site.[79] Sortase, a bacterial transpeptidase, has been used by different groups to install a variety of functionalities at the C-terminus of nanobodies, including radioisotopes (Figure 3).[77,80] Transglutaminase, lipoic acid ligase and incorporation of unnatural amino acids or terminal unpaired cysteines can likewise be used to install radioisotopes at specific sites on antibodies and antibody fragments.[81–83]

IMMUNOGENICITY AND SAFETY PROFILE OF NANOBODIES

Nanobodies have found application in preclinical and clinical studies, both as imaging agents and as therapeutics. A nanobody-based drug that targets von Willebrand factor has received approval from the US Food and Drug Administration (FDA),[84,85] and several more nanobodies are in clinical trials.[37,65,86,87] As nanobodies are derived from camelid heavy-chain-only antibodies, they can be immunogenic in humans. However, the VHH framework regions are homologous to those of human IgGs,[88,89] which may explain their low immunogenicity in clinical settings. Humanization of nanobodies is possible, and involves mutations at ~10 surface-exposed sites that render the VHH frameworks closer in sequence to that of human variable immunoglobulin domains, particularly the large VH3 subfamily.[75] However, an early clinical trial using a humanized tetravalent nanobody targeting death receptor 5 on cancer cells was stopped due to observed toxicities that were attributed to the immunogenic response.[90] Some studies suggest that nanobodies, especially the VH region, can be immunogenic in humans,[91] while others suggest that not all nanobody constructs are immunogenic.[37,65,84,92] Administration of nanobodies in doses suitable for imaging have not resulted in adverse events,[37,65] and nanobodies should therefore be considered safe. In our hands, repeated

injections of nanobodies into mice elicit an anti-VHH response in approximately half of the animals, where the response appears to be mostly specific to the particular VHH used for immunization, akin to an anti-idiotypic response. Going forward, we need to obtain a better understanding of the immunogenicity of nanobodies and the potential effect of humanization. We expect that the results emerging from ongoing nanobody-based clinical trials will help us to gain a better understanding of the immunogenicity of nanobodies.

IMAGING CANCER BIOMARKERS

Several antibodies and their fragments have advanced into clinical imaging studies, and target cancer biomarkers such as human epidermal growth factor receptor type 2 (HER2).[25,93,94] HER2 is overexpressed in 15–20% of patients with breast cancer.[95–97] HER2 is an oncogene that encodes a transmembrane tyrosine kinase receptor, and is a major therapeutic target. HER2 status is used as a classifier of invasive breast cancer.[95–97] HER2-positive breast cancers show a high incidence of metastasis with poor prognosis.[96–101] HER2-directed therapeutics, such as trastuzumab and pertuzumab, have resulted in a significant improvement in the treatment of HER2-positive cancers.[102] Analysing HER2 status on cancer cells, as done by biopsy, is therefore of immense importance. However, cancers evolve quickly, and different lesions may differ substantially from each other with respect to marker expression. Indeed, when patients with breast cancer were imaged with a full-sized immunoglobulin-based anti-HER2 agent (^{89}Zr-trastuzumab PET/CT), some patients had HER2-positive metastatic lesions and a primary tumor that was HER2-negative. These women went on to benefit from trastuzumab (Herceptin) treatment.[25] Therefore, non-invasive whole-body imaging of HER2 has already proven to be a useful adjunct to biopsies and immunostaining.

To further improve HER2-imaging abilities and to be able to perform 'same-day imaging', several groups have developed anti-HER2 nanobodies.[38,103–105] An anti-human HER2 nanobody was characterized in vivo in xenograft mouse models implanted with HER2$^+$ and HER2- human cancer cells. Using different labeling strategies, the anti-human HER2 nanobody labeled with ^{18}F, ^{131}I and ^{68}Ga detected HER2$^+$ tumors with excellent specificity.[38–40] These studies helped set the stage for clinical translation of anti-HER2 nanobodies. A phase I clinical study used the ^{68}Ga-labeled anti-HER2 nanobody to image 20 women with primary or metastatic breast carcinoma, with a HER2 immunostaining assessment of 2$^+$ or 3$^+$ (Figure 4A,B).[37] PET/CT images were obtained 10, 60 and 90 min after administration, and tracer accumulation in metastatic lesions was well above background. Primary lesions were more variable with respect to tracer accumulation, possibly due to the heterogeneous nature of the primary tumors. Overall, administration of the radiolabeled nanobody was safe and no adverse reactions were reported. The imaging agent was cleared rapidly from the circulation, with ~10% of the injected activity remaining in the circulation just 1 h post injection. Non-specific uptake was relatively high in the kidneys, liver and intestines. Further modification of the radiolabeled nanobody might reduce such non-specific uptake and improve its biodistribution profile. A phase II study is underway.

Nanobodies against other cancer biomarkers, such as epidermal growth factor receptor,[106] hepatocyte growth factor,[43] carcinoembryonic antigen[45] and HER3,[41] have been developed, radiolabeled and used in mouse models (Table 1). Overall, results from several preclinical[46–51] and early clinical imaging studies[37] show that nanobodies can be exploited as imaging agents to assess the presence or absence of important cancer biomarkers on primary tumors and metastatic lesions.

IMAGING THE EXTRACELLULAR MATRIX OF TUMORS

The ECM can be exploited to image cancer or to deliver payloads to the TME. A nanobody was developed that recognizes an alternatively spliced domain of fibronectin (fibronectin EIIIB) which is expressed in the ECM of a wide range of cancers, including melanoma, pancreatic and breast cancer.[69] The EIIIB-specific nanobody, VHH-NJB2, was radiolabeled and used to image different syngeneic and xenogeneic cancer models with primary tumors and metastatic lesions. PET using the VHH-NJB2 nanobody detected primary tumors and metastases as well as fibrotic lesions in a bleomycin-induced model.[69] The fibronectin EIIIB domain is identical in sequence in humans and mice,[69] and therefore the VHH-NJB2 nanobody detected tumors in both human and murine cancer models. Of note, the radiolabeled nanobody detected pancreatic intraepithelial neoplasias (PanINs) in KPC mice. PanINs are precursor lesions that progress to pancreatic ductal adenocarcinoma; at present, there is no alternative method to detect them. The tumor ECM presents an interesting target for further exploration in the diagnosis of metastatic lesions. Further work is needed to understand how the ECM changes in response to treatment; this information might be useful in the design of future treatment options.

IMAGING CHECKPOINT MOLECULES USING RADIOLABELED NANOBODIES

PD-L1 expression on the tumor correlates with patient survival and response to PD-1/PD-L1 blockade,[107–110] a parameter usually assessed by biopsy. However, expression of PD-L1 on cancer cells is often heterogeneous, and immunohistochemistry for PD-L1 expression has shown mixed results with respect to prognosis. Whole-body non-invasive imaging of PD-L1, which can provide visualization, localization and quantification of its expression throughout the body, is likely to be more informative and holds better prognostic value compared with immunohistochemistry. Several preclinical and clinical studies using antibodies, antibody fragments or other PD-L1-specific biomolecules, such as peptide, adnectin, affibody or PD-1 ectodomain,

1 Immunization

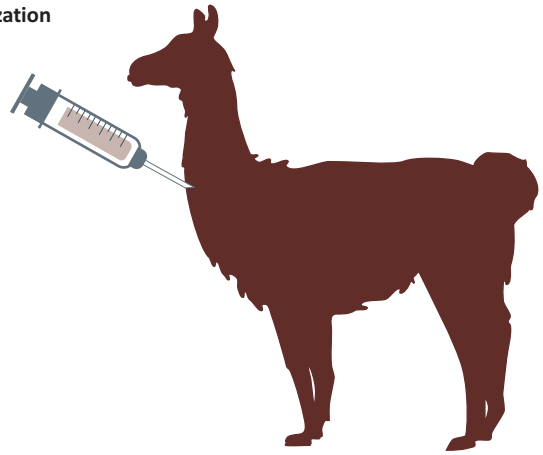

2 Isolation of lymphocytes

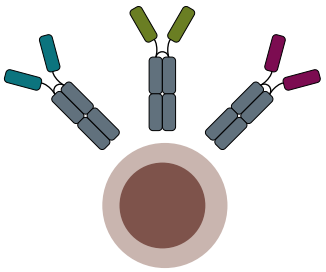

3 Amplification of VHH sequences

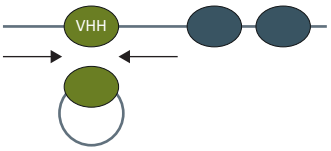

4 Construction of phage library

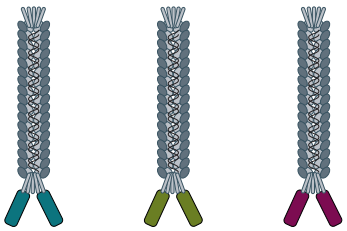

5 Panning

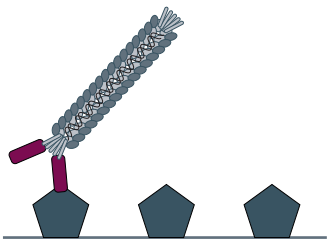

5 Expression of select VHHs

have been performed to image PD-L1 expression in tumors using non-invasive imaging techniques.[5,26,111–114]

^{89}Zr-labeled atezolizumab, an anti-PD-1 IgG antibody, was used to image patients with metastatic bladder cancer, triple-negative breast cancer and non-small cell lung cancer.[5] Images showed uptake in the spleen, liver, intestines and kidneys as the routes of clearance and metabolism of the drug. The PET signal, a function of tracer exposure and target expression, was high in lymphoid tissues and at sites of inflammation. ^{89}Zr-atezolizumab uncovered primary lesions as well as the main metastatic sites. Uptake was high in tumors but heterogeneous within and among lesions for different patients and tumor types. Tumor uptake of ^{89}Zr-atezolizumab correlated well with the patient's response to atezolizumab, and to a greater degree than clinical immunohistochemistry protocols or RNA-sequencing-based predictive biomarkers used for assessing tumor PD-L1 expression. Several other clinical PD-L1 and PD-1 imaging studies are ongoing (NCT03514719, NCT03850028, NCT04006522, NCT04222426, NCT02478099, 2019-001197-28, 2017-003511-20, NCT02760225, 2015-004260-10 and 2016-003819-36).

Smaller antibody fragments may allow same-day imaging, reduce radiation exposure and — due to higher tissue penetration capability — may reflect PD-L1 expression within and between lesions and patients more accurately. Several small molecules and antibody fragments, including nanobodies, specific for PD-L1 have been developed and used for PET. An anti-mouse PD-L1 nanobody was developed and labeled site specifically with ^{18}F.[62] PET using the ^{18}F-labeled anti-PD-L1 nanobody readily detected the B16 melanoma. In a separate study, nanobodies against murine PD-L1 were developed and labeled with ^{99m}Tc. SPECT showed that the radiolabeled anti-PD-L1 nanobodies identified PD-L1-expressing tumors but not PD-L1-negative tumors.[63]

An anti-human PD-L1 nanobody was developed and used to non-invasively image mice bearing a tumor xenograft.[64] The images showed high signal-to-noise ratios in tumors, and detected PD-L1 in melanoma and breast tumors (Figure 4C). These studies helped set the stage for translation of anti-PD-L1 nanobody into the clinic. Results from an early phase I study of a ^{99m}Tc-labeled anti-PD-L1 nanobody, performed on 16 patients with non-small cell lung cancer, were published recently.[65] No drug-related adverse events were observed. Signal was mainly detected in the kidneys, liver, spleen and bone marrow. Images revealed tumor with good signal-to-background ratios 2 h post injection, and the result correlated well with PD-L1 immunohistochemistry. Tracer uptake was shown in primary tumors, bone and nodal metastasis. The clinical trial is ongoing (NCT02978196). Whether the observed uptake in tumors and metastatic lesions correlates with the final response to the treatment remains to be seen. If successful, the ability to image patients 2 h post injection would be a remarkable advantage compared with using radiolabeled IgGs.

Table 1. Nanobodies used for non-invasive preclinical and clinical imaging

Target molecules		Stage	References
Cancer biomarkers	Human HER2	Preclinical and clinical	37–40
	Human HER3	Preclinical	41
	Human EGFR	Preclinical	42
	Human HGF	Preclinical	43
	Human CEA	Preclinical	44,45
	Human PSMA	Preclinical	46,47
	Human CD20	Preclinical	48,49
	Human Mesothelin	Preclinical	50,51
Immune markers	Murine class II MHC	Preclinical	9,52
	Human class II MHC	Preclinical	53
	Murine CD11b	Preclinical	9,54
	Murine CD8	Preclinical	54,55
	Murine MMR (CD206)	Preclinical	56,57
	Human MMR	Preclinical	57–59
	Murine Clec4F	Preclinical	60
	Murine Vsig4	Preclinical	60
	Murine CRIg	Preclinical	61
Checkpoint markers	Murine PD-L1	Preclinical	62,63
	Human PD-L1	Preclinical and clinical	64–66
	Murine CTLA-4	Preclinical	67
	Murine LAG-3	Preclinical	68
Tumor extracellular matrix	Fibronectin EIII-B (human and murine)	Preclinical	69
Cardiovascular markers	VCAM1 (human and murine)	Preclinical	70
	Murine LOX-1	Preclinical	59,71
Diabetes	Human DPP6	Preclinical	72
Amyloidosis	Human β-amyloid	Preclinical	73
	Human gelsolin	Preclinical	74

HER2, human epidermal growth factor receptor 2; HER3, human epidermal growth factor receptor 3; EGFR, epidermal growth factor receptor; HGF, hepatocyte growth factor; CEA, carcinoembryonic antigen; PSMA, prostate-specific membrane antigen; MHC, major histocompatibility complex; MMR, macrophage mannose receptor; Clec4F, C-type lectin domain family (Clec) 4 member F; Vsig4, V-set and Ig domain-containing 4; CRIg, complement receptor of the Ig superfamily; PD-L1, programmed death-ligand 1; CTLA-4, cytotoxic lymphocyte antigen-4; VCAM-1, vascular cell adhesion molecule 1; LOX-1, lectin-like oxidized low-density lipoprotein receptor-1; DPP6, dipeptidyl peptidase-like 6.

CTLA-4 is an inhibitory checkpoint molecule that is expressed constitutively on Treg cells and, to a lesser degree, on CD4 effector and CD8 cytotoxic T cells. Understanding the dynamics and distribution of the CTLA-4^{+} cells in the TME may help to improve our understanding of the tumor immune landscape and the response to treatment. A radiolabeled anti-CTLA-4 nanobody was used to non-invasively image CTLA-4 expression in a B16 melanoma model treated with anti-CTLA-4 antibody by PET.[67] Surface-accessible CTLA-4 was largely confined to the TME, with low or no signal in lymphoid organs. Several other radiolabeled anti-CTLA-4 antibodies and antibody fragments have been used in preclinical experiments.[115–117] Currently, there are

Figure 2. Generation of camelid single-domain antibodies [nanobodies or heavy-chain variable domain (VHH)]. Peripheral blood lymphocytes (PBLs) are collected following two or three rounds of immunizations. Purified PBLs are used to generate VHH phage-display libraries. Target specific nanobodies are then selected from the generated library after two or three rounds of panning. Nanobodies, expressed with appropriate tags (e.g. a sortase tag and/or a His-6 tag), are then ready for the installation of radiometal chelators or click handles.

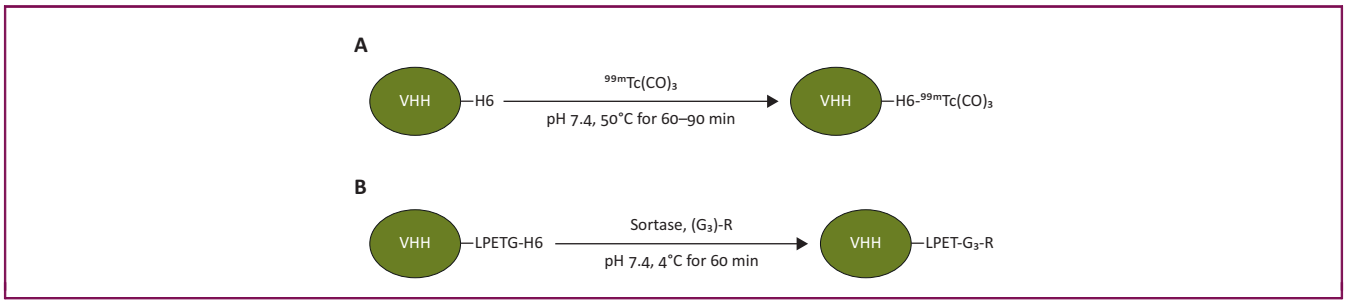

Figure 3. **(A) Direct radiolabeling of His-tagged (H6) nanobodies with ^{99m}Tc-tricarbonyl.[76] (B) Site-specific labeling of nanobodies using sortase. A nanobody equipped with an LPXTG tag can be labeled with a triglycine-containing sortase substrate. X can be a number of amino acids, such as E. A His-tag (H6) can be used to purify the protein. R can be any biomolecule of interest. Sortase reaction yields near-complete formation of product.[77,78]**

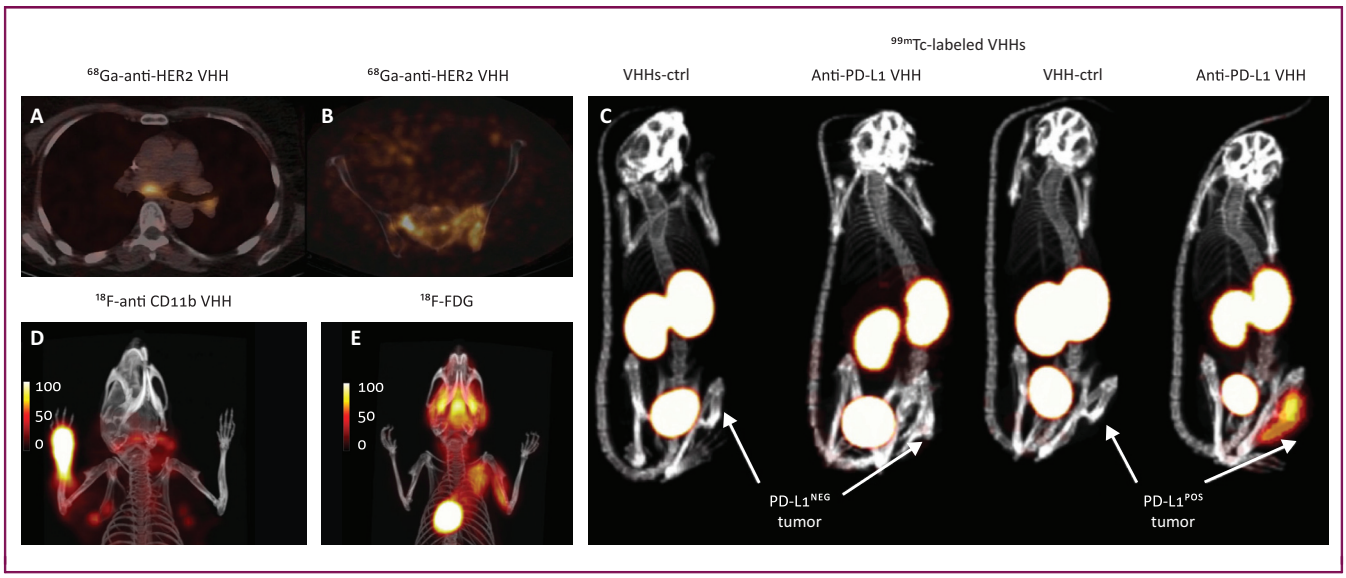

Figure 4. **(A,B) Positron emission tomography/computed tomography (PET/CT) images of ^{68}Ga-labeled anti-HER2 nanobody in patients with breast cancer showing uptake in tumor lesions. Images were obtained 90 min post injection. (A) A patient with invaded lymph nodes in the mediastinum and left hilar region. (B) A patient with bone metastasis in the pelvis. Data adapted from Keyaerts et al. (2016).[37] (C) ^{99m}Tc-labeled anti-human PD-L1 nanobody can visualize human PD-L1^{+} melanoma tumors engrafted in athymic nude mice; however, no signal was observed in PD-L1^{-} tumors. Lack of signal in the tumors when an irrelevant control nanobody was used further confirmed the specificity of the observed signal. Single-photon emission computed tomography/CT images were obtained 1 h post injection. Data adapted from Broos et al. (2019).[64] (D,E) Complete Freund's adjuvant was injected into the left paw. Twenty-four hours later, mice were imaged with ^{18}F-labeled anti-mouse CD11b nanobody, which detected an influx of CD11b^{+} cells into the site of inflammation. Lymphoid organs were also detected (~1–3% of lymphoid cells in secondary lymphoid organs are CD11b^{+}). (E) ^{18}F-2-fluoro-2-deoxyglucose (^{18}F-FDG) failed to detect the influx of CD11b^{+} cells in the same model. PET/CT images were acquired 2 h post injection of the radiolabeled heavy-chain variable domain or ^{18}F-FDG.**

Data adapted from Rashidian et al. (2015).[9]

two ongoing clinical trials using ^{89}Zr-ipilimumab, an anti-CTLA-4 IgG (NCT03313323 and 2012-003616-31). These studies will help to gain insight into how the dynamics of CTLA-4^{+} cells contribute to the antitumor immune response, and will inform whether imaging CTLA-4 holds prognostic value or not.

Lymphocyte activation gene-3 (LAG-3) (CD223) is another inhibitory checkpoint molecule on T cells.[118] Several LAG-3-targeted cancer therapies are in the clinic and many more are in preclinical development.[119] Given the importance of LAG-3, it is a potential biomarker and an important target for cancer imaging. Anti-LAG-3 nanobodies have been developed and used for non-invasive imaging.[68] The ^{99m}Tc-labeled nanobodies showed specific uptake in secondary lymphoid organs, and no signal was detected in LAG-3 knockout mice. LAG-3 expression was confirmed by flow cytometry and immunohistochemistry analyses, and correlated well with the SPECT images. Mice were inoculated subcutaneously with TC-1 mouse lung epithelial cells modified to overexpress LAG-3 and were subjected to imaging. A high specific signal was observed 1 h post injection.

Overall, nanobodies have proved to be excellent candidates for imaging of checkpoint molecules within the TME. The pharmacokinetic properties of nanobody-based imaging agents, as well as the nature of the epitopes they recognize, may be useful attributes to capture the dynamics of the checkpoint molecules and the antitumor response under immunotherapy.

IMAGING IMMUNE RESPONSES USING RADIOLABELED NANOBODIES

The myeloid compartment in the TME plays a critical role in shaping the immune landscape of tumors through cell—cell interactions and the release of soluble factors such as

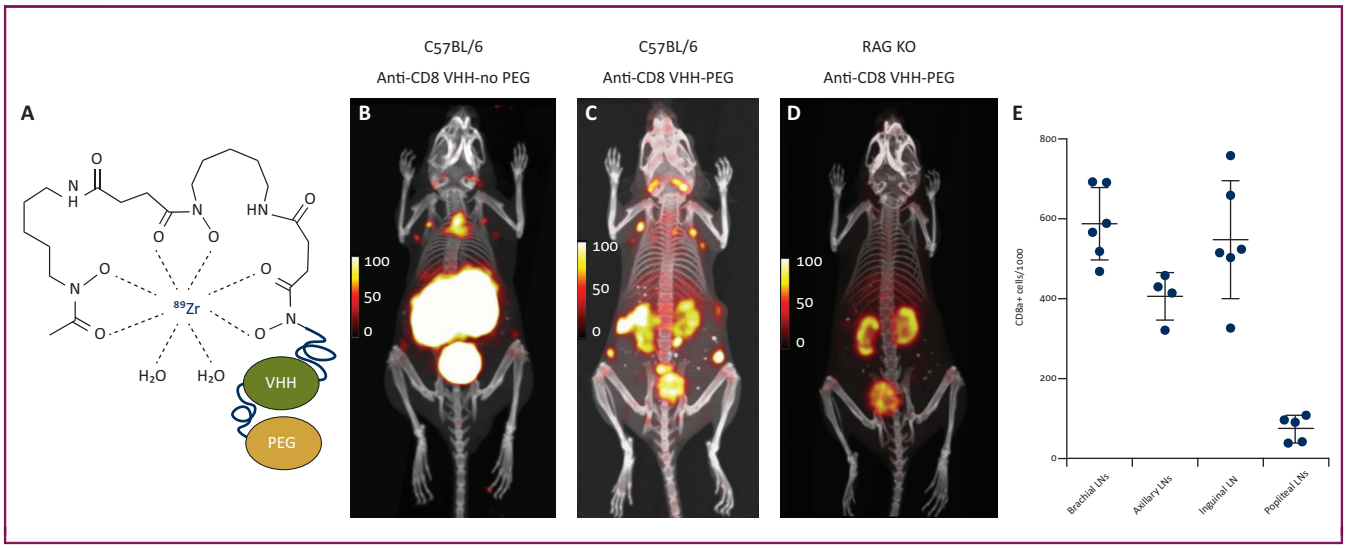

Figure 5. PEGylation increases sensitivity and decreases kidney retention of radiolabeled heavy-chain variable domains (VHHs). Mice were injected with ^{89}Zr-labeled anti-mouse CD8 nanobody (A), with or without a 20-kDa PEG molecule (B,C). Mice were imaged 2 h post injection (for the 'no PEG' VHH) or 24 h post injection (for the PEGylated VHH), which are the optimum timepoints for maximum signal-to-background ratio. RAG knockout animals, which lack all lymphocytes, did not yield an obvious signal, except in the organs of elimination (kidney, bladder) (D). To measure sensitivity of the approach, lymph nodes (LNs) were excised and CD8$^+$ cells were counted. Results showed that a popliteal LN, with ~70 000 CD8$^+$ T cells, can be detected with a signal-to-background ratio of ~7.

Data adopted from Rashidian et al. (2017, 2019).[54,55]

cytokines.[120] An antimacrophage mannose receptor (CD206) nanobody, a marker of M2-like immunosuppressive macrophages whose presence in tumors correlates with poor prognosis, detected the presence of tumor-associated macrophages in different tumor models.[56,57] Radiolabeled antimurine class II major histocompatibility complex (MHC) and CD11b nanobodies were developed to assess immune infiltrates in different tumor models.[9,52,62] The radiolabeled anticlass II MHC and anti-CD11b nanobodies were used to detect tumors in both xenogeneic and syngeneic tumor models.[9] The nanobodies detected tumors by virtue of the presence of infiltrating class II$^+$ or CD11b$^+$ immune cells. Knockout animals were used to confirm the specificity of the observed signals.[9] Imaging inflammation upon injection of complete Freund's adjuvant into the footpad of mice was also explored. The radiolabeled anti-CD11b nanobody detected inflammation in the injected paw, whereas ^{18}F-FDG did not (Figure 4D,E).

To image human immune responses, an anti-human class II MHC nanobody was developed.[53] The radiolabeled nanobody was used in a relevant humanized mouse model: NOD-SCID mice reconstituted with human fetal thymus, liver and liver-derived hematopoietic stem cells (BLT mice). These animals spontaneously develop graft-versus-host disease, characterized by alopecia and blepharitis. The radiolabeled nanobody readily detected graft-versus-host disease. In diseased animals, a significant increase in PET signal in the liver was detected, which was attributed to the infiltration of activated class II MHC$^+$ T cells. The method may thus be more generally useful to diagnose inflammation.

T cells, especially cytotoxic CD8$^+$ T cells, mediate much of the response to checkpoint blockade. The presence in biopsies of intratumoral CD8$^+$ T cells, as distinct from CD8$^+$ T cells that merely surround the tumor, correlates with a favorable response to checkpoint blockade.[6,121] Monitoring the distribution of CD8$^+$ T cells could be used to assess the response to therapy. A radiolabeled anti-CD8 nanobody was used to perform PET on mice. PET images showed label accumulation in lymphoid organs, as well as in the kidneys and bladder.[55] Addition of a PEG molecule was found to improve the efficiency of staining and decrease non-specific uptake in the kidneys (Figure 5).[55] Longitudinal imaging of CD8$^+$ T cells over time in the course of a response to CTLA-4 blockade in the B16/GVAX melanoma model was performed.[122] Images showed that so long as the CD8 PET signal was distributed homogeneously throughout the tumor, mice continued to respond and tumors did not increase in size, or did so slowly (Figure 6). When the CD8 PET signal was distributed more heterogeneously in the TME, with two or more clusters of CD8$^+$ T cells present, tumors grew faster and survival was worse (Figure 6).[55] ImmunoPET of CD8$^+$ T cells in the anti-PD-1-responsive syngeneic MC38 colorectal cancer model showed that successful PD-1 blockade is accompanied by mobilization, expansion and infiltration of cytotoxic CD8$^+$ T cells from the tumor periphery into the tumor core.[54] CD8 immunostaining on tumor samples confirmed the CD8 PET data. The different distribution patterns of CD8$^+$ T cells may thus serve as a prognostic indicator of the outcome of checkpoint blockade therapy.

Other preclinical studies have been performed to image CD8$^+$ T cells using radiolabeled antibodies. ^{89}Zr-labeled cys-diabodies (~60 kDa in size) specific for CD8 were used to monitor CD8$^+$ T-cell responses to treatment, and detected changes in the dynamics of CD8$^+$ T cells in the TME in preclinical syngeneic tumor immunotherapy models.[7,30] The images showed an acceptable signal-to-background ratio 8

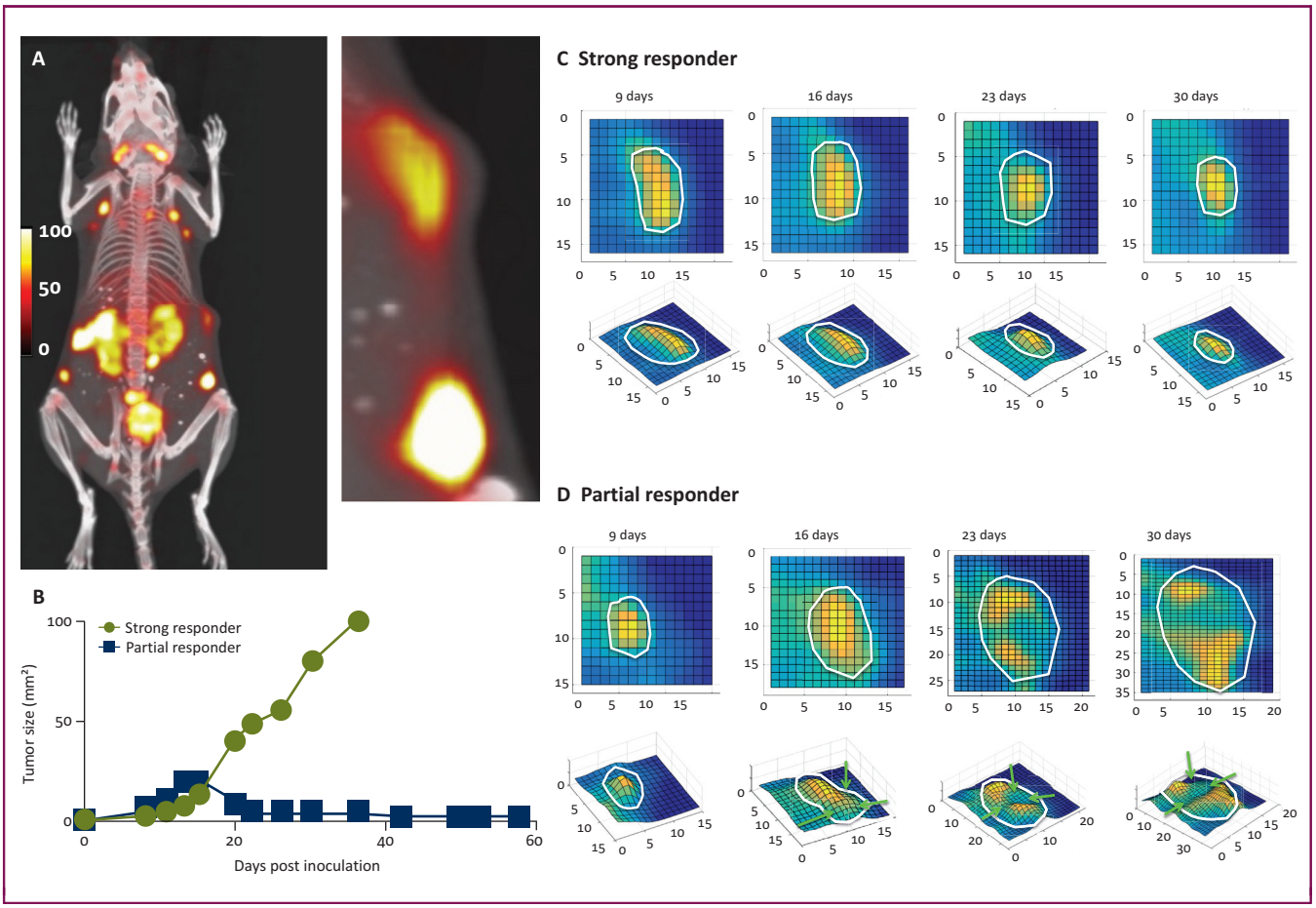

Figure 6. Monitoring the dynamics of a CD8$^+$ T-cell response to immunotherapy. (A) C57BL/6 mice were inoculated with B16 melanoma and GVAX simultaneously. Mice received anti-CTLA4 treatment (clone 9H10) in a setting that resulted in a partial response. Mice were subjected to positron emission tomography/computed tomography on days 9, 16, 23 and 30. (B) Survival graph of two mice for which PET/CT images are shown in C and D. (C,D) Images show the distribution of CD8$^+$ cells in the tumors over the course of the 4 weeks of the experiment on the indicated days. Mouse 'C' was a strong responder with homogeneous infiltration of CD8$^+$ cells throughout the course of imaging. Mouse 'D' was a partial responder. PET/CT images showed heterogeneous infiltration of CD8$^+$ cells in the tumor prior to day 23. Images are an enlarged view of two- and three-dimensional representation of a cross-section of the tumors, showing the intratumoral distribution of the PET signal. Tumors, as identified by CT, are delineated by the white outline. Where relevant, areas with lower PET signals are indicated by arrows. The images are representative of multiple experiments with similar results ($N = 20$, $P = 0.035$).

Data adapted from Rashidian et al. (2017).

h post injection, and a good signal-to-background ratio in lymphoid organs and tumors 22 h post injection, although kidney retention was relatively high, a rather common feature of immunoPET imaging agents when antibody fragments are used. An anti-human CD8 ^{89}Zr-labeled minibody was used in patients with melanoma, lung and hepatocellular carcinoma, where it was well tolerated with no adverse effects.[8] The PET images showed an acceptable signal-to-background signal in the tumors, with high uptake in the spleen, bone marrow and lymph nodes. CD8 signal in the tumor was variable and seen in approximately two-thirds of patients. ImmunoPET can thus provide information on the distribution of CD8$^+$ T cell within tumors in a clinical setting. A phase II clinical study is ongoing (NCT03802123).

These preclinical and clinical studies suggest that the distribution of CD8$^+$ T cells could serve as a biomarker of response to checkpoint blockade. Therefore, CD8 immunoPET may be useful to assess or even predict the response, or at least show a 'lack of response' to treatments.

CONCLUSION AND FUTURE DIRECTIONS

Nanobodies are excellent tools for non-invasive imaging. Desirable properties include their specificity, nanomolar to picomolar affinity, stability, fast clearance of unbound nanobody from the circulation, a pharmacokinetic and production profile compatible with short-lived radioisotopes, and ease of production. The minimal affinity required for a monovalent nanobody-based imaging agent is not known; however, for those nanobodies that have yielded acceptable images, their affinity is generally in the low nM range. High retention in the kidneys is the main drawback of nanobodies as imaging agents and may result in renal toxicities. Some nanobodies can be immunogenic, but their

immunogenicity seems to be predominantly idiotypic and specific to their variable regions. PEGylation can decrease kidney retention (Figure 5) and enhance the safety profile of radiolabeled nanobodies.[55,123,124] At the same time, PEGylation will increase circulatory half-life. Due to its very short circulatory half-life (~10 min), addition of a PEG molecule with a molecular weight <~10—20 kDa to a nanobody may still allow same-day imaging. There is a need to better understand what exactly causes a nanobody to be immunogenic and how to decrease kidney retention. The former may be specific for each nanobody, while the latter is probably a shared property.

Immunotherapy has dramatically improved the treatment of cancer, and this trend is continuing. Moving forward, we must be able to evaluate the antitumor immune responses of individual patients to immunotherapy. We need to visualize and study the specific subtype of immune cells involved before, during and after treatment so that the right treatment can be selected, or so as to allow timely modifications to treatment.

Development of additional nanobodies, and antibody fragments, is required to obtain a more comprehensive and accurate picture of the immune landscape within and around a tumor. We must be able to assess how therapeutic interventions affect this landscape. Most work thus far has focused on defining tumor-associated lymphocyte populations[125] and tumor markers.[126] Myeloid cells, including neutrophils, macrophages and dendritic cells, are important players in the immune response to cancer. Their presence and activation status help to determine the outcome of immunotherapy.[120,127] There is also an important role for innate lymphoid cells.[128] Therefore, methods to image the TME more comprehensively and identify all relevant immune cell types, as well as assessment of their functional status, are needed. Cytokines and chemokines play a major role in shaping the immune landscape of tumors.[129,130] We need to better understand the dynamics (level of presence and movement) of cytokines that play a role in shaping the TME, the identity of the cells that produce them, and when they are produced during tumor initiation and progression. Furthermore, cytokines and chemokines significantly affect, if not dictate, the phenotype of the recruited cells to be antitumor or protumor. Therefore, the ability to image the presence and distribution of certain cytokines and chemokines and their receptors may provide key information to better assess the response to treatment, or to select the right treatment at the right time for the right patient.[131,132]

The success of checkpoint blockade immunotherapy relies on the presence of tumor-specific, functional T cells.[133—135] Detection of antigen-specific T cells is critical for improved prediction or evaluation of the response to treatment. Imaging the activation status of T cells might be especially helpful in evaluating the response to a treatment. Exhausted T cells may play a lesser role in shaping the response, unless they could be returned to a more functionally active pool, the purported outcome of checkpoint blockade. Nanobodies are ideal tools to tackle many of these challenges.

While we have focused mainly on imaging applications in immuno-oncology, nanobodies have been developed to image a range of other events such as infectious disease, autoimmunity, and cardiovascular and inflammatory conditions (Table 1). Production of nanobodies is now a well-established procedure. The availability of commercial sources to perform camelid immunizations and the production of a library, including the production of synthetic nanobody libraries,[136] will continue to improve access. In addition to non-invasive imaging applications of nanobodies, there are other obvious possibilities that would benefit from their deployment, such as therapeutics or as tools for mechanistic studies in molecular and cellular biology. With several nanobodies having advanced to the clinic, and with FDA approval of one nanobody-based drug,[85] we expect this trend to continue and to see more nanobodies being developed.

FUNDING

This work was supported by the National Institutes of Health [Grant No. 1K22CA226040-01] [MR]; Innovations Research Fund at Dana-Farber Cancer Institute [MR]; National Institutes of Health [Grant No. DP1-AI150593] [HP]; Lustgarten Foundation [HP]; and Melanoma Research Alliance [HP], no grant number.

DISCLOSURE

The authors have declared no conflicts of interest.

REFERENCES

1. Topalian SL, Hodi FS, Brahmer JR, et al. Safety, activity, and immune correlates of anti—PD-1 antibody in cancer. *N Engl J Med*. 2012;366:2443—2454.
2. Leach DR, Krummel MF, Allison JP. Enhancement of antitumor immunity by CTLA-4 blockade. *Science*. 1996;271:1734—1736.
3. Couzin-Frankel J. Breakthrough of the year 2013. Cancer immunotherapy. *Science*. 2013;342:1432—1433.
4. Beer L, Hochmair M, Prosch H. Pitfalls in the radiological response assessment of immunotherapy. *Memo*. 2018;11:138—143.
5. Bensch F, van der Veen EL, Hooge MNL, et al. ^{89}Zr-atezolizumab imaging as a non-invasive approach to assess clinical response to PD-L1 blockade in cancer. *Nat Med*. 2018;24:1852—1858.
6. Callahan MK, Wolchok JD, Allison JP. Anti-CTLA-4 antibody therapy: immune monitoring during clinical development of a novel immunotherapy. *Semin Oncol*. 2010;37:473—484.
7. Tavaré R, Escuin-Ordinas H, Mok S, et al. An effective immuno-PET Imaging method to monitor CD8-dependent responses to immunotherapy. *Cancer Res*. 2016;76:73—82.
8. Pandit-Taskar N, Postow M, Hellmann M, et al. First-in-human imaging with 89Zr-Df-IAB22M2C anti-CD8 minibody in patients with solid malignancies: preliminary pharmacokinetics, biodistribution, and lesion targeting. *J Nucl Med*. 2019;61:512—519.
9. Rashidian M, Keliher EJ, Bilate AM, et al. Noninvasive imaging of immune responses. *Proc Natl Acad Sci U S A*. 2015;112:6146—6151.
10. Anaka M, Hudson C, Lo P-H, et al. Intratumoral genetic heterogeneity in metastatic melanoma is accompanied by variation in malignant behaviors. *BMC Med Genomics*. 2013;6:40.
11. Araf S, Wang J, Korfi K, et al. Genomic profiling reveals spatial intratumor heterogeneity in follicular lymphoma. *Leukemia*. 2018;32:1261—1265.
12. McGranahan N, Swanton C. Clonal heterogeneity and tumor evolution: past, present, and the future. *Cell*. 2017;168:613—628.

13. McDonald OG, Li X, Saunders T, et al. Epigenomic reprogramming during pancreatic cancer progression links anabolic glucose metabolism to distant metastasis. *Nat Genet*. 2017;49:367—376.
14. Alderton GK. Epigenetic and genetic heterogeneity in metastasis. *Nat Rev Cancer*. 2017;17:141.
15. Lawson DA, Kessenbrock K, Davis RT, Pervolarakis N, Werb Z. Tumour heterogeneity and metastasis at single-cell resolution. *Nat Cell Biol*. 2018;20:1349—1360.
16. Lear-Kaul KC, Yoon H-R, Kleinschmidt-DeMasters BK, McGavran L, Singh M. Her-2/neu status in breast cancer metastases to the central nervous system. *Arch Pathol Lab Med*. 2003;127:1451—1457.
17. Dijkers ECF, Kosterink JGW, Rademaker AP, et al. Development and characterization of clinical-grade 89Zr-trastuzumab for HER2/neu immunoPET imaging. *J Nucl Med*. 2009;50:974—981.
18. Hynes RO. The extracellular matrix: not just pretty fibrils. *Science*. 2009;326:1216—1219.
19. Blockmans D. PET in vasculitis. *Ann N Y Acad Sci*. 2011;1228:64—70.
20. Chen Y, Pullambhatla M, Foss CA, et al. 2-(3-{1-Carboxy-5-[(6-[18F] fluoro-pyridine-3-carbonyl)-amino]-pentyl}-ureido)-pentanedioic acid, [18F]DCFPyL, a PSMA-based PET imaging agent for prostate cancer. *Clin Cancer Res*. 2011;17:7645—7653.
21. Engel P, Boumsell L, Balderas R, et al. CD Nomenclature 2015: Human Leukocyte Differentiation Antigen Workshops as a Driving Force in Immunology. *J Immunol*. 2015;195:4555—4563.
22. van Dongen GAMS, Visser GWM, Lub-de Hooge MN, de Vries EG, Perk LR. Immuno-PET: a navigator in monoclonal antibody development and applications. *Oncologist*. 2007;12:1379—1389.
23. Olafsen T, Sirk SJ, Olma S, Shen CK-F, Wu AM. ImmunoPET using engineered antibody fragments: fluorine-18 labeled diabodies for same-day imaging. *Tumor Biol*. 2012;33:669—677.
24. Mayer AT, Natarajan A, Gordon SR, et al. Practical immuno-PET radiotracer design considerations for human immune checkpoint imaging. *J Nucl Med*. 2017;58:538—546.
25. Ulaner GA, Hyman DM, Ross DS, et al. Detection of HER2-positive metastases in patients with HER2-negative primary breast cancer using 89Zr-trastuzumab PET/CT. *J Nucl Med*. 2016;57:1523—1528.
26. Niemeijer AN, Leung D, Huisman MC, et al. Whole body PD-1 and PD-L1 positron emission tomography in patients with non-small-cell lung cancer. *Nat Commun*. 2018;9:1—5.
27. England CG, Jiang D, Ehlerding EB, et al. 89Zr-labeled nivolumab for imaging of T-cell infiltration in a humanized murine model of lung cancer. *Eur J Nucl Med Mol Imaging*. 2018;45:110—120.
28. Thurber GM, Schmidt MM, Wittrup KD. Antibody tumor penetration: transport opposed by systemic and antigen-mediated clearance. *Adv Drug Deliv Rev*. 2008;60:1421—1434.
29. Xenaki KT, Oliveira S, van Bergen En Henegouwen PMP. Antibody or antibody fragments: implications for molecular imaging and targeted therapy of solid tumors. *Front Immunol*. 2017;8:1287.
30. Tavare R, McCracken MN, Zettlitz KA, et al. Engineered antibody fragments for immuno-PET imaging of endogenous CD8+ T cells in vivo. *Proc Natl Acad Sci*. 2014;111:1108—1113.
31. Knowles SM, Zettlitz KA, Tavare R, et al. Quantitative immunoPET of prostate cancer xenografts with 89Zr- and 124I-labeled anti-PSCA A11 minibody. *J Nucl Med*. 2014;55:452—459.
32. Zhang Y, Hong H, Orbay H, et al. PET imaging of CD105/endoglin expression with a ^{61}/^{64}Cu-labeled Fab antibody fragment. *Eur J Nucl Med Mol Imaging*. 2013;40:759—767.
33. Chakravarty R, Goel S, Cai W. Nanobody: the "magic bullet" for molecular imaging? *Theranostics*. 2014;4:386—398.
34. Ingram JR, Schmidt FI, Ploegh HL. Exploiting nanobodies' singular traits. *Annu Rev Immunol*. 2018;36:695—715.
35. Saerens D, Muyldermans S, eds. *Single Domain Antibodies*. Totowa, NJ: Humana Press; 2012 [online]. Available at: http://www.springerlink.com/index/10.1007/978-1-61779-968-6. Accessed June 1, 2014.
36. Pardon E, Laeremans T, Triest S, et al. A general protocol for the generation of Nanobodies for structural biology. *Nat Protoc*. 2014;9:674—693.
37. Keyaerts M, Xavier C, Heemskerk J, et al. Phase I study of 68Ga-HER2-nanobody for PET/CT assessment of HER2 expression in breast carcinoma. *J Nucl Med*. 2016;57:27—33.
38. Xavier C, Blykers A, Vaneycken I, et al. 18F-nanobody for PET imaging of HER2 overexpressing tumors. *Nucl Med Biol*. 2016;43:247—252.
39. D'Huyvetter M, De Vos J, Xavier C, et al. ^{131}I-labeled anti-HER2 camelid sdAb as a theranostic tool in cancer treatment. *Clin Cancer Res*. 2017;23:6616—6628.
40. Xavier C, Vaneycken I, D'huyvetter M, et al. Synthesis, preclinical validation, dosimetry, and toxicity of 68Ga-NOTA-anti-HER2 Nanobodies for iPET imaging of HER2 receptor expression in cancer. *J Nucl Med*. 2013;54:776—784.
41. Warnders FJ, Terwisscha van Scheltinga AGT, Knuehl C, et al. Human epidermal growth factor receptor 3-specific tumor uptake and biodistribution of 89Zr-MSB0010853 visualized by real-time and noninvasive PET imaging. *J Nucl Med*. 2017;58:1210—1215.
42. Gainkam LOT, Huang L, Caveliers V, et al. Comparison of the biodistribution and tumor targeting of two 99mTc-labeled anti-EGFR nanobodies in mice, using pinhole SPECT/micro-CT. *J Nucl Med*. 2008;49:788—795.
43. Vosjan MJWD, Vercammen J, Kolkman JA, Stigter-van Walsum M, Revets H, van Dongen GAMS. Nanobodies targeting the hepatocyte growth factor: potential new drugs for molecular cancer therapy. *Mol Cancer Ther*. 2012;11:1017—1025.
44. Caveliers V, Cortez-Retamozo V, Lahoutte T, et al. 99mTc-labeled nanobodies: a new type of targeted probes for imaging antigen expression. *Curr Radiopharm*. 2008;1:37—41.
45. Vaneycken I, Govaert J, Vincke C, et al. In vitro analysis and in vivo tumor targeting of a humanized, grafted nanobody in mice using pinhole SPECT/micro-CT. *J Nucl Med*. 2010;51:1099—1106.
46. Evazalipour M, D'Huyvetter M, Tehrani BS, et al. Generation and characterization of nanobodies targeting PSMA for molecular imaging of prostate cancer: nanobody PSMA imaging. *Contrast Media Mol Imaging*. 2014;9:211—220.
47. Chatalic KLS, Veldhoven-Zweistra J, Bolkestein M, et al. A Novel 111In-labeled anti-prostate-specific membrane antigen nanobody for targeted SPECT/CT imaging of prostate cancer. *J Nucl Med*. 2015;56:1094—1099.
48. Krasniqi A, D'Huyvetter M, Xavier C, et al. Theranostic radiolabeled anti-CD20 sdAb for targeted radionuclide therapy of non-hodgkin lymphoma. *Mol Cancer Ther*. 2017;16:2828—2839.
49. Krasniqi A, Bialkowska M, Xavier C, et al. Pharmacokinetics of radiolabeled dimeric sdAbs constructs targeting human CD20. *New Biotechnol*. 2018;45:69—79.
50. Prantner AM, Turini M, Kerfelec B, et al. Anti-mesothelin nanobodies for both conventional and nanoparticle-based biomedical applications. *J Biomed Nanotechnol*. 2015;11:1201—1212.
51. Montemagno C, Bacot S, Ahmadi M, et al. Preclinical evaluation of mesothelin-specific ligands for SPECT imaging of triple-negative breast cancer. *J Nucl Med*. 2018;59:1056—1062.
52. Rashidian M, Keliher E, Dougan M, et al. The use of (18)F-2-fluorodeoxyglucose (FDG) to label antibody fragments for immuno-PET of pancreatic cancer. *ACS Cent Sci*. 2015;1:142—147.
53. Van Elssen CHMJ, Rashidian M, Vrbanac V, et al. Noninvasive imaging of human immune responses in a human xenograft model of graft-versus-host disease. *J Nucl Med*. 2017;58:1003—1008.
54. Rashidian M, LaFleur MW, Verschoor VL, et al. Immuno-PET identifies the myeloid compartment as a key contributor to the outcome of the antitumor response under PD-1 blockade. *Proc Natl Acad Sci U S A*. 2019;116:16971—16980.
55. Rashidian M, Ingram JR, Dougan M, et al. Predicting the response to CTLA-4 blockade by longitudinal noninvasive monitoring of CD8 T cells. *J Exp Med*. 2017;214:2243—2255.
56. Movahedi K, Schoonooghe S, Laoui D, et al. Nanobody-based targeting of the macrophage mannose receptor for effective *in vivo* imaging of tumor-associated macrophages. *Cancer Res*. 2012;72:4165—4177.
57. Blykers A, Schoonooghe S, Xavier C, et al. PET imaging of macrophage mannose receptor—expressing macrophages in tumor stroma using

18F-radiolabeled camelid single-domain antibody fragments. *J Nucl Med*. 2015;56:1265—1271.
58. Bala G, Baudhuin H, Remory I, et al. Evaluation of [99mTc]radiolabeled macrophage mannose receptor-specific nanobodies for targeting of atherosclerotic lesions in mice. *Mol Imaging Biol*. 2018;20:260—267.
59. Senders ML, Hernot S, Carlucci G, et al. Nanobody-facilitated multiparametric PET/MRI phenotyping of atherosclerosis. *JACC Cardiovasc Imaging*. 2019;12:2015—2026.
60. Zheng F, Sparkes A, De Baetselier P, et al. Molecular imaging with Kupffer cell-targeting nanobodies for diagnosis and prognosis in mouse models of liver pathogenesis. *Mol Imaging Biol*. 2017;19:49—58.
61. Zheng F, Put S, Bouwens L, et al. Molecular imaging with macrophage CRIg-targeting nanobodies for early and preclinical diagnosis in a mouse model of rheumatoid arthritis. *J Nucl Med*. 2014;55:824—829.
62. Ingram JR, Dougan M, Rashidian M, et al. PD-L1 is an activation-independent marker of brown adipocytes. *Nat Commun*. 2017;8:647.
63. Broos K, Keyaerts M, Lecocq Q, et al. Non-invasive assessment of murine PD-L1 levels in syngeneic tumor models by nuclear imaging with nanobody tracers. *Oncotarget*. 2017;8:41932—41946.
64. Broos K, Lecocq Q, Xavier C, et al. Evaluating a single domain antibody targeting human PD-L1 as a nuclear imaging and therapeutic agent. *Cancers*. 2019;11:872.
65. Xing Y, Chand G, Liu C, et al. Early phase I study of a 99mTc-labeled anti—programmed death ligand-1 (PD-L1) single-domain antibody in SPECT/CT assessment of PD-L1 expression in non—small cell Lung cancer. *J Nucl Med*. 2019;60:1213—1220.
66. Lv G, Sun Y, Qiu L, et al. PET imaging of tumor PD-L1 expression with a highly specific non-blocking nanobody. *J Nucl Med*. 2020;61:117—122.
67. Ingram JR, Blomberg OS, Rashidian M, et al. Anti-CTLA-4 therapy requires an Fc domain for efficacy. *Proc Natl Acad Sci U S A*. 2018;115:3912—3917.
68. Lecocq Q, Zeven K, De Vlaeminck Y, et al. Noninvasive imaging of the immune checkpoint LAG-3 using nanobodies, from development to pre-clinical use. *Biomolecules*. 2019;9:548.
69. Jailkhani N, Ingram JR, Rashidian M, et al. Noninvasive imaging of tumor progression, metastasis, and fibrosis using a nanobody targeting the extracellular matrix. *Proc Natl Acad Sci U S A*. 2019;116:14181—14190.
70. Broisat A, Hernot S, Toczek J, et al. Nanobodies targeting mouse/human VCAM1 for the nuclear imaging of atherosclerotic lesions. *Circ Res*. 2012;110:927—937.
71. De Vos J, Mathijs I, Xavier C, et al. Specific targeting of atherosclerotic plaques in ApoE(-/-) mice using a new Camelid sdAb binding the vulnerable plaque marker LOX-1. *Mol Imaging Biol*. 2014;16:690—698.
72. Balhuizen A, Massa S, Mathijs I, et al. A nanobody-based tracer targeting DPP6 for non-invasive imaging of human pancreatic endocrine cells. *Sci Rep*. 2017;7:15130.
73. Nabuurs RJA, Rutgers KS, Welling MM, et al. In vivo detection of amyloid-β deposits using heavy chain antibody fragments in a transgenic mouse model for Alzheimer's disease. *PLoS One*. 2012;7:e38284.
74. Verhelle A, Van Overbeke W, Peleman C, et al. Non-invasive imaging of amyloid deposits in a mouse model of AGel using 99mTc-modified nanobodies and SPECT/CT. *Mol Imaging Biol*. 2016;18:887—897.
75. Vincke C, Loris R, Saerens D, Martinez-Rodriguez S, Muyldermans S, Conrath K. General strategy to humanize a camelid single-domain antibody and identification of a universal humanized nanobody scaffold. *J Biol Chem*. 2009;284:3273—3284.
76. Xavier C, Devoogdt N, Hernot S, et al. Site-specific labeling of his-tagged nanobodies with ^{99}mTc: a practical guide. *Methods Mol Biol*. 2012;911:485—490.
77. Crauwels M, Massa S, Martin C, et al. Site-specific radioactive labeling of nanobodies. *Methods Mol Biol*. 2018;1827:505—540.
78. Pishesha N, Ingram JR, Ploegh HL. Sortase A: a model for transpeptidation and its biological applications. *Annu Rev Cell Dev Biol*. 2018;34:163—188.
79. Rashidian M, Dozier JK, Distefano MD. Enzymatic labeling of proteins: techniques and approaches. *Bioconjug Chem*. 2013;24:1277—1294.
80. Guimaraes CP, Witte MD, Theile CS, et al. Site-specific C-terminal and internal loop labeling of proteins using sortase-mediated reactions. *Nat Protoc*. 2013;8:1787—1799.
81. Jeger S, Zimmermann K, Blanc A, et al. Site-specific and stoichiometric modification of antibodies by bacterial transglutaminase. *Angew Chem Int Ed*. 2010;49:9995—9997.
82. Drake CR, Sevillano N, Truillet C, Craik CS, VanBrocklin HF, Evans MJ. Site-specific radiofluorination of biomolecules with 8-[(18)F]-fluorooctanoic acid catalyzed by lipoic acid ligase. *ACS Chem Biol*. 2016;11:1587—1594.
83. Adumeau P, Sharma SK, Brent C, Zeglis BM. Site-specifically labeled immunoconjugates for molecular imaging—part 2: peptide tags and unnatural amino acids. *Mol Imaging Biol*. 2016;18:153—165.
84. Bartunek J, Barbato E, Heyndrickx G, Vanderheyden M, Wijns W, Holz J-B. Novel antiplatelet agents: ALX-0081, a nanobody directed towards von Willebrand factor. *J Cardiovasc Transl Res*. 2013;6:355—363.
85. Morrison C. Nanobody approval gives domain antibodies a boost. *Nat Rev Drug Discov*. 2019;18:485—487.
86. Steeland S, Vandenbroucke RE, Libert C. Nanobodies as therapeutics: big opportunities for small antibodies. *Drug Discov Today*. 2016;21:1076—1113.
87. Debie P, Devoogdt N, Hernot S. Targeted nanobody-based molecular tracers for nuclear imaging and image-guided surgery. *Antibodies*. 2019;8:12.
88. Klarenbeek A, El Mazouari K, Desmyter A, et al. Camelid Ig V genes reveal significant human homology not seen in therapeutic target genes, providing for a powerful therapeutic antibody platform. *mAbs*. 2015;7:693—706.
89. Muyldermans S. Nanobodies: natural single-domain antibodies. *Annu Rev Biochem*. 2013;82:775—797.
90. Papadopoulos KP, Isaacs R, Bilic S, et al. Unexpected hepatotoxicity in a phase I study of TAS266, a novel tetravalent agonistic Nanobody® targeting the DR5 receptor. *Cancer Chemother Pharmacol*. 2015;75:887—895.
91. Holland MC, Wurthner JU, Morley PJ, et al. Autoantibodies to variable heavy (VH) chain Ig sequences in humans impact the safety and clinical pharmacology of a VH domain antibody antagonist of TNF-α receptor 1. *J Clin Immunol*. 2013;33:1192—1203.
92. Detalle L, Stohr T, Palomo C, et al. Generation and characterization of ALX-0171, a potent novel therapeutic nanobody for the treatment of respiratory syncytial virus infection. *Antimicrob Agents Chemother*. 2016;60:6—13.
93. Dijkers EC, Oude Munnink TH, Kosterink JG, et al. Biodistribution of 89Zr-trastuzumab and PET imaging of HER2-positive lesions in patients with metastatic breast cancer. *Clin Pharmacol Ther*. 2010;87:586—592.
94. Tamura K, Kurihara H, Yonemori K, et al. 64Cu-DOTA-trastuzumab PET imaging in patients with HER2-positive breast cancer. *J Nucl Med*. 2013;54:1869—1875.
95. Ross JS, Slodkowska EA, Symmans WF, Pusztai L, Ravdin PM, Hortobagyi GN. The HER-2 receptor and breast cancer: ten years of targeted anti-HER-2 therapy and personalized medicine. *Oncologist*. 2009;14:320—368.
96. Loibl S, Gianni L. HER2-positive breast cancer. *Lancet*. 2017;389:2415—2429.
97. Wolff AC, Hammond MEH, Hicks DG, et al. Recommendations for human epidermal growth factor receptor 2 testing in breast cancer: American Society of Clinical Oncology/College of American Pathologists clinical practice guideline update. *Arch Pathol Lab Med*. 2014;138:241—256.
98. Znidaric T, Gugic J, Marinko T, et al. Breast cancer patients with brain metastases or leptomeningeal disease: 10-year results of a national cohort with validation of prognostic indexes. *Breast J*. 2019;25:1117—1125.
99. Lin NU. Brain metastases in HER2-positive breast cancer. *Lancet Oncol*. 2013;14:185—186.

100. Martin AM, Cagney DN, Catalano PJ, et al. Brain metastases in newly diagnosed breast cancer: a population-based study. *JAMA Oncol*. 2017;3:1069–1077.
101. Kennecke H, Yerushalmi R, Woods R, et al. Metastatic behavior of breast cancer subtypes. *J Clin Oncol*. 2010;28:3271–3277.
102. Olson EM, Abdel-Rasoul M, Maly J, Wu CS, Lin NU, Shapiro CL. Incidence and risk of central nervous system metastases as site of first recurrence in patients with HER2-positive breast cancer treated with adjuvant trastuzumab. *Ann Oncol*. 2013;24:1526–1533.
103. D'Huyvetter M, Vincke C, Xavier C, et al. Targeted radionuclide therapy with A (177)Lu-labeled anti-HER2 nanobody. *Theranostics*. 2014;4:708–720.
104. Pruszynski M, D'Huyvetter M, Bruchertseifer F, Morgenstern A, Lahoutte T. Evaluation of an anti-HER2 nanobody labeled with ^{225}Ac for targeted α-particle therapy of cancer. *Mol Pharm*. 2018;15:1457–1466.
105. Jamnani FR, Rahbarizadeh F, Shokrgozar MA, Ahmadvand D, Mahboudi F, Sharifzadeh Z. Targeting high affinity and epitope-distinct oligoclonal nanobodies to HER2 over-expressing tumor cells. *Exp Cell Res*. 2012;318:1112–1124.
106. Leung K. (89)Zr-Desferrioxamine p-isothiocyanatobenzyl-anti-EGFR nanobody 7D12. In: *Molecular Imaging and Contrast Agent Database (MICAD)*. Bethesda (MD): National Center for Biotechnology Information (US); 2004. Available at: http://www.ncbi.nlm.nih.gov/books/NBK97356/. Accessed June 15, 2014.
107. Schmidt LH, Kümmel A, Görlich D, et al. PD-1 and PD-L1 Expression in NSCLC Indicate a Favorable Prognosis in Defined Subgroups. *PLoS One*. 2015;10:e0136023.
108. Cooper WA, Tran T, Vilain RE, et al. PD-L1 expression is a favorable prognostic factor in early stage non-small cell carcinoma. *Lung Cancer*. 2015;89:181–188.
109. Passiglia F, Bronte G, Bazan V, et al. PD-L1 expression as predictive biomarker in patients with NSCLC: a pooled analysis. *Oncotarget*. 2016;7:19738–19747.
110. Davis AA, Patel VG. The role of PD-L1 expression as a predictive biomarker: an analysis of all US Food and Drug Administration (FDA) approvals of immune checkpoint inhibitors. *J Immunother Cancer*. 2019;7:278.
111. Chatterjee S, Lesniak WG, Miller MS, et al. Rapid PD-L1 detection in tumors with PET using a highly specific peptide. *Biochem Biophys Res Commun*. 2017;483:258–263.
112. Kumar D, Lisok A, Dahmane E, et al. Peptide-based PET quantifies target engagement of PD-L1 therapeutics. *J Clin Invest*. 2019;129:616–630.
113. Jagoda EM, Vasalatiy O, Basuli F, et al. Immuno-PET imaging of the programmed cell death-1 ligand (PD-L1) using a zirconium-89 labeled therapeutic antibody, avelumab. *Mol Imaging*. 2019;18, 1536012119829986.
114. Donnelly DJ, Smith RA, Morin P, et al. Synthesis and biologic evaluation of a novel ^{18} F-Labeled adnectin as a PET radioligand for imaging PD-L1 expression. *J Nucl Med*. 2018;59:529–535.
115. Higashikawa K, Yagi K, Watanabe K, et al. 64Cu-DOTA-anti-CTLA-4 mAb enabled PET visualization of CTLA-4 on the T-cell infiltrating tumor tissues. *PLoS One*. 2014;9:e109866.
116. Ehlerding EB, England CG, Majewski RL, et al. ImmunoPET imaging of CTLA-4 expression in mouse models of non-small cell lung cancer. *Mol Pharm*. 2017;14:1782–1789.
117. Ehlerding EB, Lee HJ, Jiang D, et al. Antibody and fragment-based PET imaging of CTLA-4+ T-cells in humanized mouse models. *Am J Cancer Res*. 2019;9:53–63.
118. Goldberg MV, Drake CG. LAG-3 in Cancer Immunotherapy. In: Dranoff G, ed. *Cancer Immunology and Immunotherapy*. 344. Berlin, Heidelberg: Springer Berlin Heidelberg; 2010:269–278.
119. Andrews LP, Marciscano AE, Drake CG, Vignali DAA. LAG3 (CD223) as a cancer immunotherapy target. *Immunol Rev*. 2017;276:80–96.
120. DeNardo DG, Andreu P, Coussens LM. Interactions between lymphocytes and myeloid cells regulate pro- versus anti-tumor immunity. *Cancer Metastasis Rev*. 2010;29:309–316.
121. Pardoll DM. The blockade of immune checkpoints in cancer immunotherapy. *Nat Rev Cancer*. 2012;12:252–264.
122. Quezada SA, Peggs KS, Curran MA, Allison JP. CTLA4 blockade and GM-CSF combination immunotherapy alters the intratumor balance of effector and regulatory T cells. *J Clin Invest*. 2006;116:1935–1945.
123. Rashidian M, Wang L, Edens JG, et al. Enzyme-mediated modification of single-domain antibodies for imaging modalities with different characteristics. *Angew Chem Int Ed Engl*. 2016;55:528–533.
124. Harris JM, Chess RB. Effect of pegylation on pharmaceuticals. *Nat Rev Drug Discov*. 2003;2:214–221.
125. Hendry S, Salgado R, Gevaert T, et al. Assessing tumor-infiltrating lymphocytes in solid tumors: a practical review for pathologists and proposal for a standardized method from the International Immunooncology Biomarkers Working Group: part 1: assessing the host immune response, TILs in invasive breast carcinoma and ductal carcinoma in situ, metastatic tumor deposits and areas for further research. *Adv Anat Pathol*. 2017;24:235–251.
126. Nagpal M, Singh S, Singh P, Chauhan P, Zaidi MA. Tumor markers: a diagnostic tool. *Natl J Maxillofac Surg*. 2016;7:17–20.
127. Mills CD, Lenz LL, Harris RA. A breakthrough: macrophage-directed cancer immunotherapy. *Cancer Res*. 2016;76:513–516.
128. Moral JA, Leung J, Rojas LA, et al. ILC2s amplify PD-1 blockade by activating tissue-specific cancer immunity. *Nature*. 2020;579:130–135.
129. Lee S, Margolin K. Cytokines in cancer immunotherapy. *Cancers*. 2011;3:3856–3893.
130. Smyth MJ, Cretney E, Kershaw MH, Hayakawa Y. Cytokines in cancer immunity and immunotherapy. *Immunol Rev*. 2004;202:275–293.
131. Di Gialleonardo V, Signore A, Glaudemans AWJM, Dierckx RAJO, De Vries EFJ. N-(4-18F-fluorobenzoyl)interleukin-2 for PET of human-activated T lymphocytes. *J Nucl Med*. 2012;53:679–686.
132. Hartimath SV, Draghiciu O, van de Wall S, et al. Noninvasive monitoring of cancer therapy induced activated T cells using [18F]FB-IL-2 PET imaging. *Oncoimmunology*. 2017;6:e1248014.
133. Gubin MM, Zhang X, Schuster H, et al. Checkpoint blockade cancer immunotherapy targets tumour-specific mutant antigens. *Nature*. 2014;515:577–581.
134. Alspach E, Lussier DM, Miceli AP, et al. MHC-II neoantigens shape tumour immunity and response to immunotherapy. *Nature*. 2019;574:696–701.
135. Schumacher TN, Schreiber RD. Neoantigens in cancer immunotherapy. *Science*. 2015;348:69–74.
136. Moutel S, Bery N, Bernard V, et al. NaLi-H1: a universal synthetic library of humanized nanobodies providing highly functional antibodies and intrabodies. *eLife*. 2016;5:e16228.